EDGE ARTICLE

Check for updates

Four-step continuous-flow total synthesis of (−)-debromoflustramine B using a chiral heterogeneous Pd NP catalyst†

Junwen Wang,‡[a] Feng Liang,‡[a] Zhen Dong,[a] Junrong Huang, [a] Yuxiang Zhu, *[d] Hengzhi You *[ab] and Fen-Er Chen *[abc]

Various prenylated indoline alkaloids with diverse biological activities, including (−)-debromoflustramine B with significant butyrylcholinesterase inhibitory activity, could be synthesized by dearomative prenylation reactions of tryptophan derivatives. However, previously reported dearomative prenylations were limited to batch reactions at the milligram scale, requiring multistep reactions and complex post-processing to obtain the desired natural products. The more efficient synthesis of alkaloids remains challenging, as does the recovery of expensive catalysts. Herein, we developed a chiral heterogeneous Pd nanoparticle (NP) catalyst supported on a polymer, which produces indoline alkaloids in high yields with excellent enantioselectivities. Additionally, the first gram-scale four-step continuous-flow total synthesis of (−)-debromoflustramine B was successfully achieved with this chiral Pd heterogeneous catalyst, requiring only a simple post-processing step.

Introduction

Dearomative prenylation reactions of tryptophan derivatives produce prenylated indoline alkaloids, featuring a skeleton of hexahydropyrrolo[2,3-*b*]indole with diverse biological activities (Fig. 1A).[1–4] Well-known natural products with such a skeleton include flustramines isolated from the bryozoa *Flustra foliacea* and (−)-debromoflustramine B, which contain significant butyrylcholinesterase inhibitory activity,[5–7] potentially offering curative effects for Alzheimer's disease.[8] Therefore, the total synthesis of these compounds has received great attention in the field of pharmaceutical chemistry (Fig. 1B). In the past two decades, total synthesis of (−)-flustramine B and (−)-debromoflustramine B has been well developed using three different approaches: (i) asymmetric non-metal catalysis including iminium,[9] bisguanidinium,[10] chiral phosphoric acid (CPA),[11] and phosphine[12] catalyzed synthesis; (ii) asymmetric metal catalysis including Ru,[13] Ir,[14] and Pd[15,16] catalyzed synthesis; (iii) chiral auxiliary-assisted synthesis, such as the use of chiral sulfinyl

[a]School of Science, Harbin Institute of Technology (Shenzhen), 518055, China. E-mail: youhengzhi@hit.edu.cn; rfchen@fudan.edu.cn

[b]Green Pharmaceutical Engineering Research Center, Harbin Institute of Technology (Shenzhen), Shenzhen, 518055, China

[c]Engineering Center of Catalysis and Synthesis for Chiral Molecules, Department of Chemistry, Fudan University, Shanghai, 200433, China

[d]School of Pharmaceutical Sciences (Shenzhen), Shenzhen Campus of Sun Yat-sen University, Shenzhen, 518107, China. E-mail: zhuyx86@mail.sysu.edu.cn

† Electronic supplementary information (ESI) available. See DOI: https://doi.org/10.1039/d4sc03471f

‡ These authors contributed equally.

amides.[17] Although numerous synthetic methods have been developed,[18] these processes are still confined to multistep reactions at a small scale and require tedious post-processing. Furthermore, the recovery of expensive catalysts in the above syntheses remains challenging since homogeneous catalysts were employed.

Combining continuous-flow technology with heterogeneous catalysts provides tremendous advantages over conventional batch reactions in terms of reaction efficiency, scalability, safety, environmental friendliness[19–23] and catalyst recovery.[24–26] Besides these practical advantages, successful employment of heterogeneous catalysts in packed-bed reactors[27,28] under flow processes further demonstrates their merits in line with the green chemistry concept and catalyst recovery. Additionally, the multistep continuous-flow total synthesis can achieve better efficiency by avoiding the tedious post-processing and the isolation of intermediates,[29] realizing automated processes in synthetic chemistry. Therefore, developing a heterogeneous catalyst for the synthesis of prenylated indoline alkaloids under continuous-flow conditions holds significant importance in terms of step economy and column economy. This paves the way for feasible industrial-scale production, which benefits the ongoing research and the clinical application of these natural products.

Even though excellent pioneering studies on heterogeneous catalysts have been reported,[30–40] cases employing multistep continuous-flow conditions for the synthesis of natural products remain a key challenge. Following our previous work on a chiral heterogeneous Cu NP catalyst,[41] we have developed a chiral heterogeneous Pd NP catalyst supported on a polymer.
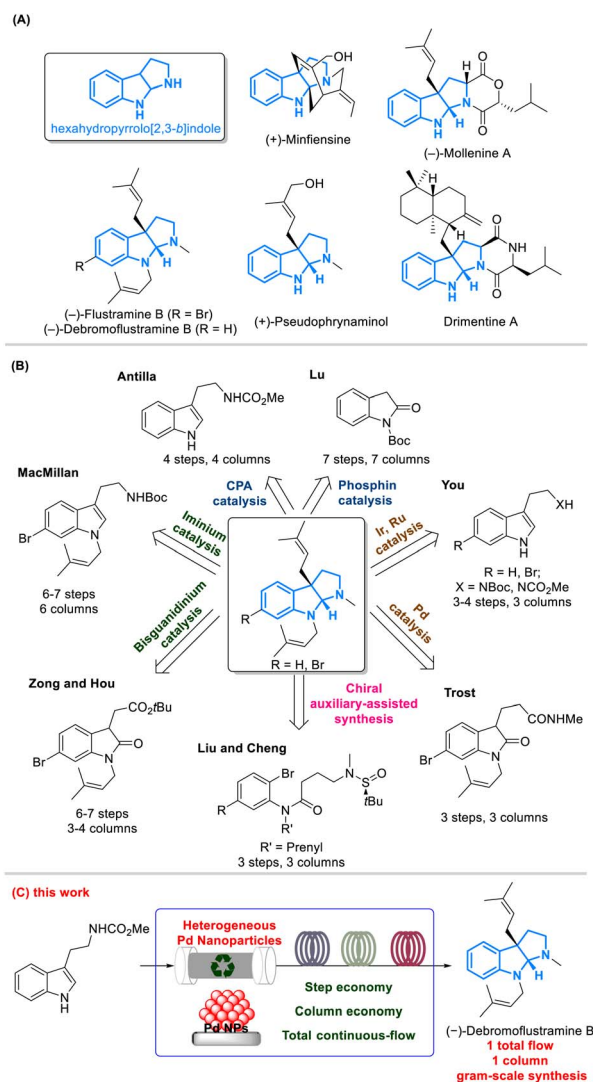
Fig. 1 (A) Representative indoline alkaloids with a hexahydropyrrolo[2,3-*b*] indole skeleton; (B) reported asymmetric syntheses of (−)-debromoflustramine B and (−)-flustramine B; (C) Pd NP enabled multistep continuous-flow total synthesis of (−)-debromoflustramine B.

This Pd NP catalyst exhibits excellent durability and maintains its activity compared to its homogeneous counterpart, leading to the production of various indoline alkaloids in high yields with excellent enantioselectivities. In addition, we have accomplished the first four-step continuous-flow total synthesis of (−)-debromoflustramine B on a gram scale (Fig. 1C). Importantly, there is no need for tedious post-processing or isolation of intermediates, as only one column chromatography step is required to obtain the optically pure product.

Results and discussion

Catalyst synthesis and catalyst characterization

The chiral heterogeneous Pd NP catalyst was prepared using a modified procedure described in our previous work.[41] The catalyst synthesis began with the installation of a styrene substituent on the BINOL skeleton, leading to the production of

the phosphoramidite monomer **M1**, which was then subjected to simple polymerization conditions to obtain the polymer. Lastly, the Pd NP catalyst was prepared by complexation of the polymer and a homogeneous palladium source (Fig. 2A). The Pd/ligand ratio was found to be approximately 2 : 1, as confirmed by ICP-OES analysis (Pd, 19.3%, 1.82 mmol g^{-1}; P, 3.09%, 1 mmol g^{-1}) of the Pd NP catalyst.

To confirm and elucidate the interior structure of the heterogeneous Pd NP catalyst, comprehensive characterization studies were performed. The X-ray diffraction (XRD) patterns of the polymer (Fig. S1†) and Pd NPs (Fig. S2†) indicated that both are highly polymerized and amorphous. Connected peaks observed in solid-state ^{13}C NMR spectra ranging from 127.87 to 149.99 ppm for the polymer and 128.18 to 148.60 ppm for the Pd NPs indicated the presence of aromatic rings in both. Similarly, peaks at 65.05/48.41 ppm for the polymer and 65.25/48.93 ppm for Pd NPs suggested the presence of an N-allyl substituent in both. Additionally, the characteristic peaks of the vinyl group in monomer **M1** ranging from 110 to 120 ppm disappeared, and strong connected peaks from 22.59 to 40.05 ppm (polymer) and 22.78 to 40.69 ppm (Pd NPs) appeared, suggesting the successful polymerization of monomer **M1** and immobilization of the chiral vinylbenzyl-substituted phosphoramidite ligands respectively (Fig. 2B). In solid-state ^{31}P NMR spectra of the polymer and Pd NPs, peaks observed at 146.23 ppm and 153.91 ppm[15] were similar to the peak in monomer **M1**, suggesting that the active centers (phosphorus) of chiral ligands remain stable after polymerization and coordination (Fig. 2C).

In FT-IR spectra, the characteristic absorption bands of polystyrene (PS) at 2924 and 2847 cm^{-1} were also presented in the polymer and Pd NPs. In addition, similar connected peaks ranging from 900 to 1330 cm^{-1} in monomer **M1** were observed in the polymer and Pd NPs, indicating successful
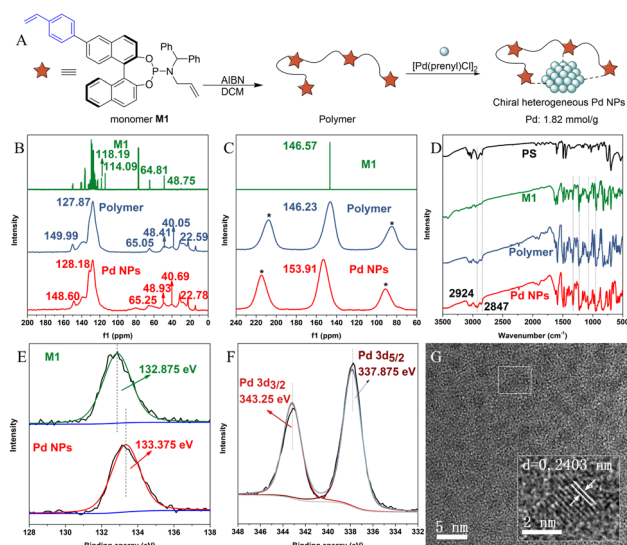

Fig. 2 Catalyst synthesis and characterization. (A) Synthesis of the chiral Pd NP catalyst; (B) solid state ^{13}C NMR spectra of **M1**, the polymer, and Pd NPs; (C) solid state ^{31}P NMR spectra of **M1**, the polymer, and Pd NPs; (D) FT-IR spectra of PS, **M1**, the polymer and Pd NPs; (E) P 2p of XPS analysis for **M1** and Pd NPs; (F) Rh 3d of XPS analysis for Pd NPs; (G) TEM of Pd NPs.

polymerization and coordination. This finding is consistent with the above conclusion (Fig. 2D). To better understand the coordination environment of the Pd NPs, X-ray photoelectron spectroscopy (XPS) analysis was conducted. The spectra showed the successful coordination of the palladium atom to the phosphorus atoms, as supported by the shift (0.5 eV) in binding energies between P 2p of monomer **M1** and Pd NPs (Fig. 2E). Moreover, the metal species in Pd NPs was confirmed to be palladium using the spectra of Pd 3d (Fig. 2F).[42] Energy dispersive X-ray spectroscopy (EDS) and transmission electron microscopy (TEM) of Pd NPs (Fig. S8†) were also performed to confirm the uniform distribution of the P, S, and Pd elements over the Pd NPs. Clear lattices were found uniformly in the image of TEM of Pd NPs (Fig. 2G), which contain a lattice spacing of 0.2403 nm (2.403 Å), similar to the average Pd–Pd distance[43] (2.38 Å) in Pd NPs. In summary, the above characterization studies confirmed the successful and uniform immobilization of Pd atoms with the polymer and the desired coordination environment of the Pd atoms with the ligands.

Activity evaluation

This chiral heterogeneous Pd NP catalyst was first evaluated for enantioselective dearomative prenylation of tryptophan derivatives **1a** under batch conditions at a 0.1 mmol scale (Table S1†). It was revealed that this Pd NP catalyst was applicable with excellent immobilization efficiency, enabling the production of desired alkaloid **3a** in high yield (95%) with excellent enantioselectivity (91% ee).

Substrate scope

With the optimized reaction conditions in hand, we further investigated the scope of the reaction. The Pd NP catalyst was confirmed to have excellent functional group tolerance to a series of tryptophan derivatives in enantioselective dearomative prenylation (Fig. 3). In the case of employing NHCO₂Me as the nucleophile, both electron-deficient (Br-substituted) and electron-rich (OMe-substituted) tryptamines tolerated the system and gave products **3b** and **3c** in good yields (75–97%) with excellent enantioselectivities (89–90% ee). Substrates with different N-protecting groups, such as CO₂Et, CO₂^iPr, *tert*-butoxycarbonyl (Boc), cyclopentoxycarbonyl and benzyloxycarbonyl (Cbz), also delivered excellent results (**3d–3i**, 74–99% yields with 90–93% ee). Moreover, using a flavoring agent and pharmaceutically useful ʟ-menthol (−) menthyl oxycarbonyl as the N-protecting group yielded product **3j** in 84% yield with 96% ee. Even the natural hormone melatonin and its derivate were readily transformed into the desired products **3k** and **3l** in excellent yields (88% yield for both) with excellent enantioselectivities (89–90% ee). Additionally, substrates possessing an alcohol nucleophile and a carbon (diester) nucleophile were able to produce the desired products **3m–3o** with good yields and enantioselectivities (81–90% yields, 82–91% ee).

Multistep continuous-flow

The batch recycling experiment revealed Pd leaching during the catalyst recovery process. This occurred as the aqueous NH₄Cl

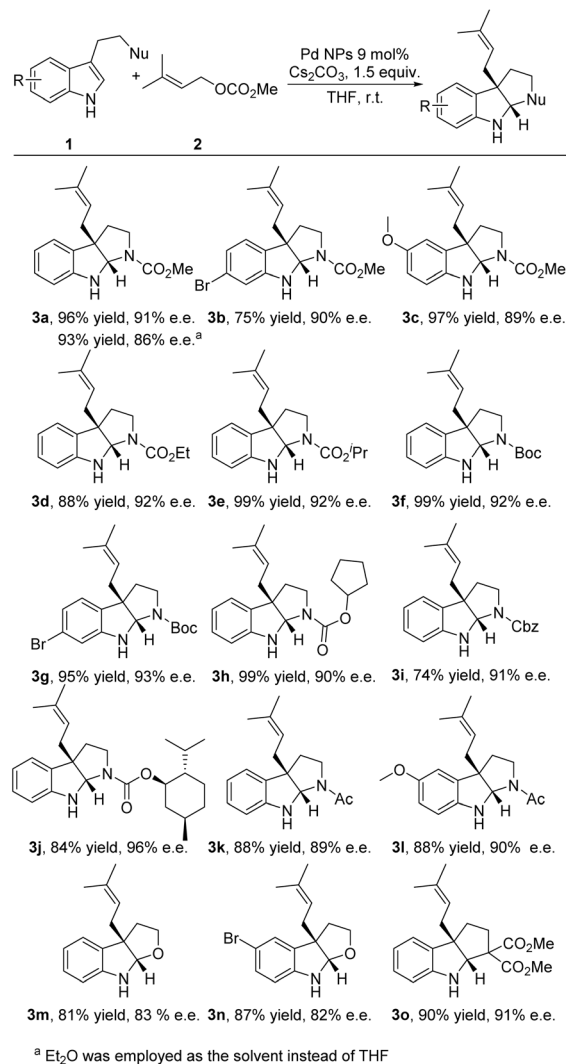**Fig. 3** Scope of the Pd NP catalyzed dearomative prenylation.

solution removed both Cs₂CO₃ and Pd from the catalyst (Tables S2 and S3†). Consequently, we believe that the flow process, which eliminates the need for post-processing, could be a more viable solution. To elucidate the versatility of the Pd NP catalyst and develop a more step- and column-economical approach for the synthesis of (−)-debromoflustramine B, a four-step continuous-flow process was developed, which required only one column chromatography step (Fig. 4). Although employing heterogeneous catalysts in packed-bed reactors provides numerous benefits, there are also problems such as system incompatibility in multistep natural product synthesis. To solve this problem, we improved the synthetic circuit by dividing it into four flow pathways. First, tryptophan derivatives **1a** (0.6 M in Et₂O,[44] 1 equiv.) and methyl prenyl carbonate **2** (0.9 M in Et₂O,[44] 1.5 equiv.) were pumped into a column packed-bed reactor containing the chiral heterogeneous Pd NP catalyst and Cs₂CO₃ at the same velocity (15 μL min⁻¹) in flow 1, leading to the production of prenylated indoline alkaloid **3a** (Fig. 4), flow 1. Upon generation of **3a**, it was premixed with *t*BuOK
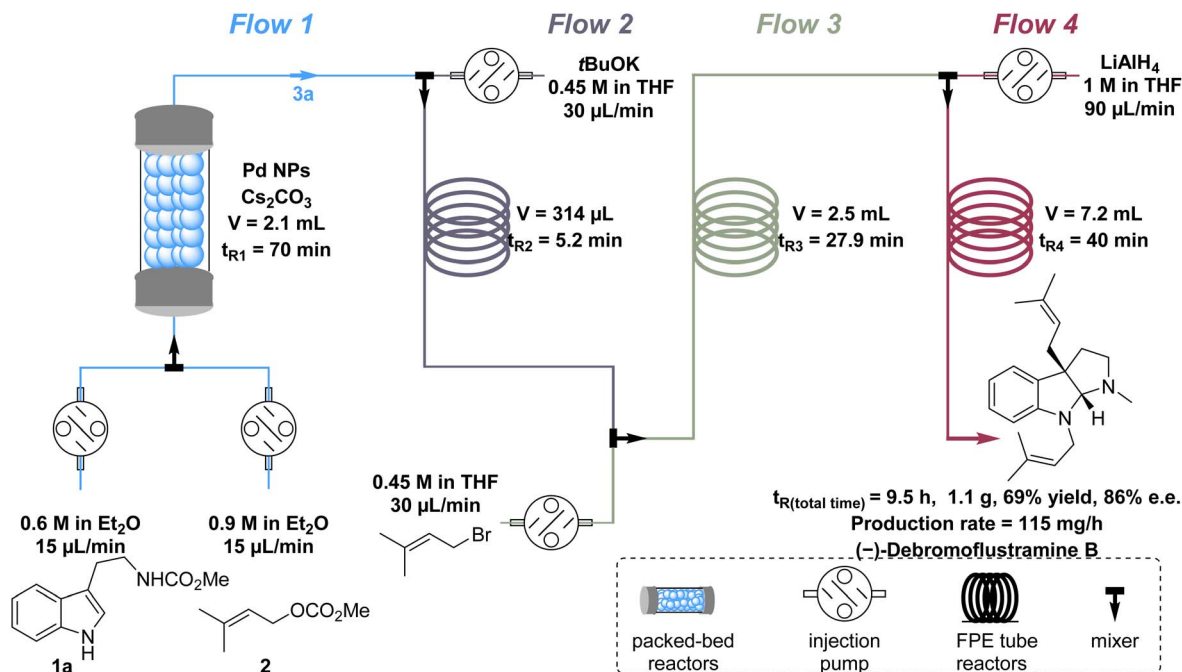
Fig. 4 The four-step continuous-flow total synthesis of (−)-debromoflustramine B.

(0.45 M in THF, 1.5 equiv., 30 μL min^{-1}) in an FEP tube for 5 min in flow 2 before being mixed in flow 3 with prenyl bromide (0.45 M in THF, 1.5 equiv., 30 μL min^{-1}) to afford the precursor of (−)-debromoflustramine B. Subsequent reduction with LiAlH$_4$ (1 M in THF, 10 equiv., 90 μL min^{-1}) in flow 4 delivered the desired natural product (−)-debromoflustramine B on a gram scale (1.1 g). The product was obtained with an overall yield of 69% and complete retention of the enantiomeric purity (86% ee). It was worth noting that this process would produce solid blockage in the flow path. Therefore, a FEP tube with a large inner diameter was conducive to the process, and ultrasonic treatment was performed in the flow path to further prevent clogging. This four-step continuous-flow total synthesis method not only avoids multistep reactions and post-processing, but also enhances synthesis efficiency through improved step and column economy. Additionally, the catalyst can be easily recovered once the process is completed.

Conclusions

In conclusion, we have elaborated the design and synthesis of an efficient polymer-supported chiral Pd NP catalyst for the enantioselective dearomative prenylation of tryptophan derivatives. The comprehensive characterization studies of the catalyst revealed that it is a highly polymerized matrix with well-distributed active catalytic centers. Meanwhile, the first four-step continuous-flow total synthesis of (−)-debromoflustramine B on a gram scale was successfully achieved, producing the desired product in 69% yield with 86% ee over 4 steps. Notably, the process requires only one multistep continuous-flow process and one column chromatography step, compared to the previously reported 3–7-step synthesis with at least 3

column chromatography steps. This work demonstrates the potential of developing an efficient heterogeneous catalyst for asymmetric catalysis, and its application in continuous flow systems offers a more efficient and industrially friendly solution for large-scale natural product synthesis.

Data availability

The data supporting this article have been included as part of the ESI.†

Author contributions

J. W. and F. L. conducted the experiments and prepared the ESI;† Z. D. helped synthesize catalysts. J. H. contributed to the discussion. J. W. and Y. Z. designed the experiments and wrote the manuscript. H. Y. and F. C. directed the project. All the authors contributed to this work.

Conflicts of interest

There are no conflicts to declare.

Acknowledgements

Notes and references

1 T. Lindel, N. Marsch and S. K. Adla, in *Alkaloid Synthesis*, ed. H.-J. Knölker, Springer, Berlin, Heidelberg, 2012, pp. 67–129.
2 S.-M. Li, *Nat. Prod. Rep.*, 2009, **27**, 57–78.
3 R. M. Williams, E. M. Stocking and J. F. Sanz-Cervera, in *Biosynthesis: Aromatic Polyketides, Isoprenoids, Alkaloids*, eds. F. J. Leeper and J. C. Vederas, Springer, Berlin, Heidelberg, 2000, pp. 97–173.
4 Y.-Z. Liu, H. Song, C. Zheng and S.-L. You, *Nat. Synth.*, 2022, **1**, 203–216.
5 P. B. Holst, U. Anthoni, C. Christophersen and P. H. Nielsen, *J. Nat. Prod.*, 1994, **57**, 997–1000.
6 J. S. Carle and C. Christophersen, *J. Am. Chem. Soc.*, 1979, **101**, 4012–4013.
7 E. Rivera-Becerril, P. Joseph-Nathan, V. M. Pérez-Álvarez and M. S. Morales-Ríos, *J. Med. Chem.*, 2008, **51**, 5271–5284.
8 S. Zhou and G. Huang, *Biomed. Pharmacother.*, 2022, **146**, 112556.
9 J. F. Austin, S.-G. Kim, C. J. Sinz, W.-J. Xiao and D. W. C. MacMillan, *Proc. Natl. Acad. Sci. U. S. A.*, 2004, **101**, 5482–5487.
10 X. Zuo, Z. Wan, Z. Liao, C. Wang, C.-H. Tan, S. Huo and L. Zong, *ACS Catal.*, 2023, **13**, 15708–15714.
11 Z. Zhang and J. C. Antilla, *Angew. Chem., Int. Ed.*, 2012, **51**, 11778–11782.
12 X. Tang, H. Ni and Y. Lu, *Org. Chem. Front.*, 2021, **8**, 4485–4489.
13 X. Zhang, Z.-P. Yang, C. Liu and S.-L. You, *Chem. Sci.*, 2013, **4**, 3239–3243.
14 X. Zhang, L. Han and S.-L. You, *Chem. Sci.*, 2014, **5**, 1059–1063.
15 H.-F. Tu, X. Zhang, C. Zheng, M. Zhu and S.-L. You, *Nat. Catal.*, 2018, **1**, 601–608.
16 B. M. Trost, S. Malhotra and W. H. Chan, *J. Am. Chem. Soc.*, 2011, **133**, 7328–7331.
17 X. Shen, T. Peng, F. Wang, S. Li, X. Lei, W. Yunxiao, F. Cheng and T. Liu, *ChemistrySelect*, 2021, **6**, 5195–5197.
18 C. Zheng and S.-L. You, *Nat. Prod. Rep.*, 2019, **36**, 1589–1605.
19 J. Liao, S. Zhang, Z. Wang, X. Song, D. Zhang, R. Kumar, J. Jin, P. Ren, H. You and F.-E. Chen, *Green Synth. Catal.*, 2020, **1**, 121–133.
20 J. Britton and T. F. Jamison, *Angew. Chem., Int. Ed.*, 2017, **56**, 8823–8827.
21 C. Liu, J. Xie, W. Wu, M. Wang, W. Chen, S. B. Idres, J. Rong, L.-W. Deng, S. A. Khan and J. Wu, *Nat. Chem.*, 2021, **13**, 451–457.
22 B. Gutmann, J.-P. Roduit, D. Roberge and C. O. Kappe, *Angew. Chem., Int. Ed.*, 2010, **49**, 7101–7105.
23 T. Tsubogo, T. Ishiwata and S. Kobayashi, *Angew. Chem., Int. Ed.*, 2013, **52**, 6590–6604.
24 M. Movsisyan, E. I. P. Delbeke, J. K. E. T. Berton, C. Battilocchio, S. V. Ley and C. V. Stevens, *Chem. Soc. Rev.*, 2016, **45**, 4892–4928.
25 Y. Saito and S. Kobayashi, *Angew. Chem., Int. Ed.*, 2021, 202112797.
26 G. Laudadio, Y. Deng, K. van der Wal, D. Ravelli, M. Nuño, M. Fagnoni, D. Guthrie, Y. Sun and T. Noël, *Science*, 2020, **369**, 92–96.
27 S. Cañellas, C. Ayats, A. H. Henseler and M. A. Pericàs, *ACS Catal.*, 2017, **7**, 1383–1391.
28 J. Lai, M. Fianchini and M. A. Pericàs, *ACS Catal.*, 2020, **10**, 14971–14983.
29 T. Tsubogo, H. Oyamada and S. Kobayashi, *Nature*, 2015, **520**, 329–332.
30 T. Kuremoto, T. Yasukawa and S. Kobayashi, *Adv. Synth. Catal.*, 2019, **361**, 3698–3703.
31 T. Kuremoto, R. Sadatsune, T. Yasukawa and S. Kobayashi, *ACS Catal.*, 2021, 14026–14031.
32 Y. Saito and S. Kobayashi, *Angew. Chem., Int. Ed.*, 2024, **63**, e202313778.
33 Y. Otomaru, T. Senda and T. Hayashi, *Org. Lett.*, 2004, **6**, 3357–3359.
34 G. Shen, T. Osako, M. Nagaosa and Y. Uozumi, *J. Org. Chem.*, 2018, **83**, 7380–7387.
35 W.-Y. Huang, G.-Q. Wang, W.-H. Li, T.-T. Li, G.-J. Ji, S.-C. Ren, M. Jiang, L. Yan, H.-T. Tang, Y.-M. Pan and Y.-J. Ding, *Chem*, 2020, **6**, 2300–2313.
36 V. B. Saptal, V. Ruta, M. A. Bajada and G. Vilé, *Angew. Chem., Int. Ed.*, 2023, **62**, e202219306.
37 W.-H. Li, J. Yang, D. Wang and Y. Li, *Chem*, 2022, **8**, 119–140.
38 M. A. Bajada, J. Sanjosé-Orduna, G. D. Liberto, S. Tosoni, G. Pacchioni, T. Noël and G. Vilé, *Chem. Soc. Rev.*, 2022, **51**, 3898–3925.
39 Z. Chen, E. Vorobyeva, S. Mitchell, E. Fako, M. A. Ortuño, N. López, S. M. Collins, P. A. Midgley, S. Richard, G. Vilé and J. Pérez-Ramírez, *Nat. Nanotechnol.*, 2018, **13**, 702–707.
40 H. Ishitani, K. Kanai, W. Yoo, T. Yoshida and S. Kobayashi, *Angew. Chem., Int. Ed.*, 2019, **58**, 13313–13317.
41 J. Wang, J. Li, Y. Wang, S. He, H. You and F.-E. Chen, *ACS Catal.*, 2022, **12**, 9629–9637.
42 P. Brant, L. S. Benner and A. L. Balch, *Inorg. Chem.*, 1979, **18**, 3422–3427.
43 G. Liu, W. Zhou, Y. Ji, B. Chen, G. Fu, Q. Yun, S. Chen, Y. Lin, P.-F. Yin, X. Cui, J. Liu, F. Meng, Q. Zhang, L. Song, L. Gu and H. Zhang, *J. Am. Chem. Soc.*, 2021, **143**, 11262–11270.
44 Due to the gradual dissolution of Pd NPs in THF, Et$_2$O was employed in the multistep continuous flow synthesis.